

# Boundary effects for weakly driven polymers

J. M. J. VAN LEEUWEN\*† and ANDRZEJ DRZEWIŃSKI‡§

†Instituut-Lorentz, University of Leiden, PO Box 9506, 2300 RA Leiden, The Netherlands

‡Czestochowa University of Technology, Institute of Mathematics and Computer Science,  
ul.Dabrowskiego 73, 42-200 Czestochowa, Poland

§Institute of Low Temperature and Structure Research, Polish Academy of Sciences,  
PO Box 1410, 50-950 Wrocław 2, Poland

(Received 19 April 2005; in final form 5 May 2005)

We consider an arbitrarily charged polymer driven by a weak electric field through a gel. The orientation of these polymers can be derived from a central model in which only the head is charged. The orientation displays characteristic bulk and tail behaviour. The form of the scaling laws are derived and the scaling functions have been determined numerically. The paper deals with the physical mechanisms of the orientation profile near the tail of the polymer and clarifies why mean field approximations utterly fail in understanding the dynamics of long polymers.

## 1. Introduction

Polymer motion seems to have unsurmountable complications for a theoretically inclined physicist. It is one of the achievements of Ben Widom to have made this field attractive for theoretical physicists [1]. A number of simplifying steps have to be made in order to make the problem tractable. De Gennes launched the idea of reptation [2]. The simplest illustration of reptation is the motion of polymers dissolved in a gel. A gel is a rigid structure of pores. The polymer traces out a sequence of pores (the tube [3]) and slithers through the tube as a reptile, accumulating length in one pore and then transports it to an adjacent pore along the tube. The ends of the polymer may find new pores, thus extending the tube, or retracting from the pore and so shortening the tube. In a solution, polymers often obtain a charge per unit base pair, which allows a polymer to drive them through the gel with an electric field. This is gel electrophoresis, a widely used technique in DNA fingerprinting. The biased diffusive motion gives a net drift of the polymer in the direction of the field. The drift velocity is sensitive to the length of the polymer, which is exploited in selecting DNA fragments according to their length.

A second simplifying step is to convert the dynamics into a stochastic process, since detailed molecular

dynamics will be restricted to rather short polymers, while the theoretical interest is in the scaling behaviour, i.e. the way in which the length of the polymers enters in the properties for asymptotically long polymers. This simplification is obtained by the notion of ‘reptons’. A repton (or Kuhn’s unit) is a group of base pairs of the order of the persistence length. As a consequence the motion of successive reptons is virtually uncorrelated. A gel like agarose has pores that are so large that they can accommodate several reptons. So the tube may be seen as a chain of pores which are all occupied by at least one repton. The polymer dynamics is then reduced to a stochastic hopping of reptons to adjacent pores. The reptons are connected by links, which are either taut (connecting reptons in different pores) or slack (connecting reptons in the same pore). They hop independently from each other with the only proviso that the integrity of the polymer is preserved, which means that the pores along the tube always have a non-zero occupation. Thus sufficient length has to be stored before a repton can move. This is the idea of reptation: an alternating process of accumulation of stored length inside a pore and diffusion of this stored length to neighbouring pores.

The third simplification was made by Rubinstein by discretizing space into a set of cells [4]. For convenience the cells are arranged in a regular lattice. This looks like a crude approximation, but the one-dimensional structure of the polymer implies that practically only the coordination number of the pores matters and even that has no influence on the universal properties like

\*Corresponding author. Email: [jmjvanl@lorentz.leidenuniv.nl](mailto:jmjvanl@lorentz.leidenuniv.nl)

scaling exponents. Duke [5] accounted for the electric driving field by giving hops in the field direction a bias over the hops against the field. After all these simplifications it seems that the model has little to do anymore with the reality. But Barkema and co-workers [6, 7] showed that the model, in spite of its simplicity, still describes surprisingly well the basic properties of polymer motion in a gel.

Simplicity is an understatement for the Rubinstein–Duke (RD) model. Since Widom popularized the model, the exact solution of the model has so far defied vigorous attempts. The major reason is that boundary effects play an essential role. Tube renewal at the ends of the polymers induces two regimes: the bulk of the polymer and boundary regions, of the order of  $N^{1/2}$ , where  $N$  is the number of links. The academic case of a periodically repeating polymer is exactly soluble [8, 9], but its connection to the real problem is limited to the leading term in the drift velocity [10]. The more technical reason for the difficulties is the lack of detailed balance in the master equation for the stochastic process. Thus there is no systematic procedure for obtaining the solution. However, the solution seemed within reach for a while, because in the past decade, great progress was made in the so-called asymmetric exclusion models [11]. One can phrase the RD model also in terms of particles hopping along a 1-dimensional chain, with asymmetric rates and mutually excluding each other [12]. The difficulty, however, is that one needs two types of particles together with vacancies and no useful matrix product representation exists for this variant. So one must rely on numerical methods. The obvious candidate is the Monte Carlo technique and Barkema *et al.* [6] performed extensive simulations, revealing interesting scaling properties. There is, however, a drawback in using Monte Carlo techniques for the RD model, since the renewal time increases as  $N^3$ , which makes simulations increasingly slow for long polymers.

The present authors have exploited the analogy of the master equation with the Schrödinger equation for one-dimensional quantum problems. White has developed a density matrix method (DMRG) [13, 14], which gives, when applied to the reptation problem, amazingly accurate data for medium length chains [15–17]. The lengths, which we extended to  $N \simeq 150$ , are not fully in the asymptotic regime. But the solution technique gradually builds up the chain, leading to accurate data for a sequence of lengths up to  $N \simeq 150$ . These data are

ideally suited for finite size analysis and therefore the results can be extended to arbitrarily long chains via the scaling forms.

In a previous paper [18] we established a relation between the various ways in which the hopping can be biased. This allows one to express the probability distribution in terms of that of the chosen model. We take the so-called magnetophoresis (MP) variant [19, 20] in which the force is only exerted on the head repton of the chain. Both the original RD model as well as the MP variant have been extensively studied by the DMRG method. The method not only gives the global properties as the drift velocity and the renewal time, but also detailed information about the orientation and some nearby correlations of the chain. We have shown that scaling relations exist for the rather involved orientation profile. Orientation and drift are intimately related, since there is a direct relation between the orientation of the end links and the drift velocity.

In this paper we use the map of the orientation on the probability density of a tagged particle diffusing along the chain, in order to explain the physical mechanism leading to the typical orientation profiles of a reptating chain. The diffusing tagged particle builds up algebraically decaying correlations, rendering mean-field approximations useless in predicting the orientation in the RD model. We start the paper with a short description of the model and the map of the various realizations onto each other. In addition we indicate the way in which the orientation can be obtained from a random walk interpretation. We show that the hopping rates for the random walker cannot meaningfully be derived from a mean-field approximation. We derive the form of the scaling laws from a few principles and extend the numerical data to higher embedding dimensions. We then analyse the physics behind the algebraic decay of the correlations and present an approximate scheme to calculate the hopping rates.

## 2. Rubinstein–Duke related models

For the description of the RD model we refer to Widom *et al.* [1]. The reptons are numbered from 0 to  $N$  and are connected by  $N$  links, which are mapped on a vector  $\mathbf{y}$ , consisting of variables  $y_1, \dots, y_N$ , each of which can take the values 1, 0 or  $-1$ . We count from tail (link 1) to head (link  $N$ )<sup>†</sup>. The non-zero  $y_j$  are the taut links and  $y_j = 0$  corresponds to a slack link. The basic processes are interchanges of a 0 with either 1 or  $-1$ . They represent

<sup>†</sup>This convention differs from previous papers, where  $N$  is the number of reptons. Since the  $N$  links are the basic variables, we have decided to break with this unnatural tradition.

diffusion of stored length to the neighbouring cell. At the tail of the chain  $y_1 = 0$  can turn into a  $y_1 = \pm 1$  representing an extension of the tube. Their transition rate gets a factor  $d$ , where  $d$  is the embedding dimension. This corresponds to the  $d$  possible neighbour cells to which the tail repton may move. The reverse process, changing  $y_1 = \pm 1$  into  $y_1 = 0$ , does not carry this factor, since shortening of the tube can only occur in one way. At the head of the chain similar transitions involve  $y_N$ . The master equation for the stationary probability distribution  $P(\mathbf{y})$  can be cast in the form

$$\sum_{\mathbf{y}'} [W(\mathbf{y}|\mathbf{y}')P(\mathbf{y}') - W(\mathbf{y}'|\mathbf{y})P(\mathbf{y})] \equiv \mathcal{M}P(\mathbf{y}) = 0. \quad (1)$$

$W(\mathbf{y}|\mathbf{y}')$  is the transition rate from configuration  $\mathbf{y}'$  to  $\mathbf{y}$ . The reptons are electrically charged and the hops are biased by an electric field. A move of repton  $j$  has a bias

$$W(\mathbf{y}|\mathbf{y}') = B_i = \exp(q_i \epsilon / 2). \quad (2)$$

$q_i$  is the charge of repton  $i$  and  $\epsilon$  is a measure for the field strength.  $\epsilon \ll 1$  is a small parameter in this paper. Hops of repton  $i$  in the direction of the field are encouraged by this factor  $B_i$  and those against the field discouraged by the factor  $B_i^{-1}$ .

We expand the master equation (1) in powers of  $\epsilon$

$$\mathcal{M} = \mathcal{M}^0 + \epsilon \mathcal{M}^1 + \dots, \quad P(\mathbf{y}) = P^0(\mathbf{y}) + \epsilon P^1(\mathbf{y}) + \dots, \quad (3)$$

leading to the hierarchy of equations

$$\begin{cases} \mathcal{M}^0 P^0 = 0, \\ \mathcal{M}^0 P^1 + \mathcal{M}^1 P^0 = 0. \end{cases} \quad (4)$$

The first equation involves the zeroth order master operator, which results by replacing all the  $B_j$  by 1. As in the embedding  $d$ -dimensional lattice, all realizations are equally probable since the first equation (4) has the normalized solution

$$P^0(\mathbf{y}) = \frac{d^{L(\mathbf{y})}}{(2d+1)^N}, \quad L(\mathbf{y}) = \sum_{j=1}^N y_j^2, \quad (5)$$

with  $L(\mathbf{y})$  the length of the confining tube.

There is no technique, other than numerical, to solve the second equation (4). However a surprising relation exists between the solutions for various charge distributions  $q_i$ . It can be shown that [18]

$$P^1(\mathbf{y}) = P_\phi(\mathbf{y}) + (N+1)P_{\text{MP}}^1(\mathbf{y}), \quad (6)$$

with the definition

$$P_\phi(\mathbf{y}) = \sum_{j=1}^N \phi_j y_j P^0(\mathbf{y}). \quad (7)$$

$\phi_j$  is recursively defined as

$$\phi_1 = -q_0, \quad \phi_{j+1} - \phi_j = -q_j \quad \text{for } j = 1, \dots, N-1. \quad (8)$$

From (6) the full probability for an arbitrary charge distribution is expressed by a special one,  $P_{\text{MP}}^1(\mathbf{y})$ , satisfying the equation

$$\mathcal{M}^0 P_{\text{MP}}^1(\mathbf{y}) + \bar{q} y_N P^0(\mathbf{y}) = 0, \quad (9)$$

with  $\bar{q}$  the average charge of the chain

$$\bar{q} = \frac{1}{N+1} \sum_{i=0}^N q_i. \quad (10)$$

Clearly (9) refers to a problem where the chain is pulled by the head repton only. It is indicated by the subscript MP, which is an abbreviation for *magnetophoresis*. A realization of this case is a magnetic bead attached to a neutral polymer, which is pulled by a magnetic force. So we take the MP model as the central model, from which the properties of other models can be constructed using (6). In fact the MP model is simpler to understand than a chain with an arbitrary distribution of charges. One obvious advantage of the MP model is that the chain is always *oriented*. Pulling at the head repton gives on average a chain where the head is also the foremost repton.

In the original Rubinstein–Duke model all the charges are equal. We refer to this case as the electrophoresis (EP) model. As a special case of (6) we have the connection between the EP and the MP model

$$P_{\text{EP}}^1(\mathbf{y}) = - \sum_{j=1}^N j q y_j P^0(\mathbf{y}) + (N+1)P_{\text{MP}}^1(\mathbf{y}), \quad (11)$$

where the corresponding MP system has the same charge  $q$  on the head repton (standardly one sets  $q = 1$  in the EP model).

The EP problem has a head–tail symmetry, implying the relation

$$P_{\text{EP}}^1(\mathbf{y}) = P_{\text{EP}}^1(\mathbf{y}^T), \quad (12)$$

where  $\mathbf{y}^T$  is the transposed configuration  $\mathbf{y}^T = (-y_N, \dots, -y_1)$ . Inserting (12) into (11) yields for  $P_{\text{MP}}^1(\mathbf{y})$

$$P_{\text{MP}}^1(\mathbf{y}) = P_{\text{MP}}^1(\mathbf{y}^T) + \sum_{j=1}^N y_j P^0(\mathbf{y}). \quad (13)$$

Relation (6) suggests, writing to first order,  $P^1(\mathbf{y})$  as

$$P^1(\mathbf{y}) = \sum_{j=1}^N y_j \Phi_j(\mathbf{y}). \quad (14)$$

This seems an overkill in introducing variables, since we have  $N$  functions  $\Phi_j(\mathbf{y})$ , each of which could depend on the full  $3^N$  configurations. However the advantage of (14) is that  $\Phi_j$  only depends on the values of  $y_j^2$ . Due to the linearization in the field the two link values  $y_j = \pm 1$  have become equivalent. In order to express this in the notation, we introduce the variables  $x_j = y_j^2$ . In view of a subsequent new interpretation we call a taut link ( $x_j = 1$ ) a particle and a slack link ( $x_j = 0$ ) a hole. Thus  $\Phi_j$  is a function  $\Phi_j(\mathbf{x})$ . As  $\Phi_j(\mathbf{x})$  only has meaning for  $x_j = 1$ , we set its value for  $x_j = 0$  equal to 0. For the MP model we write

$$P_{\text{MP}}^1(\mathbf{y}) = \sum_{j=1}^N y_j P_j(\mathbf{x}), \quad (15)$$

using again the symbol  $P$  on the right-hand side, since it has been shown that  $P_j(\mathbf{x})$  can be seen as the probability on the configuration  $(j, \mathbf{x})$ . It obeys a master equation with a slightly different transition matrix. One may view the index  $j$  in  $P_j$  as a tag on the link  $j$ . As before, particles can only interchange with neighbouring holes, not with each other. There is, however, permanently only one tagged particle present. At the end of the chain, particles may be created or annihilated, but there are no moves of a tagged particle in or out of the chain. The only process that is added is the reversal of the configuration when the tag is at the tail (not at the head). This gives the picture of a tagged particle starting at the head and diffusing through the chain (without bias) towards the tail. Once it has arrived at the tail the configuration may flip and the tagged particle starts its diffusive process again at the head.

Since we are mostly interested in the local orientation we transform the relation

$$\langle y_j \rangle = \sum_{\mathbf{y}} y_j P(\mathbf{y}) \quad (16)$$

into an expression in terms of the probability  $p_j$  the probability that the tagged particle is at link  $j$  as

$$p_j = \sum_{\mathbf{x}} P_j(\mathbf{x}), \quad \langle y_j \rangle_{\text{MP}} = \frac{2d}{2d+1} p_j. \quad (17)$$

The behaviour of  $p_j$  is the focus of this paper.

### 3. Mean-field approximation

In lowest order in  $\varepsilon$  the orientation vanishes; so we concentrate on the first-order contribution. According to relation (6) the orientation of an arbitrary charged chain can be related to that of the MP chain as

$$\langle y_j \rangle / \varepsilon = -\phi_j \frac{2d}{2d+1} + (N+1) \langle y_j \rangle_{\text{MP}} / \varepsilon. \quad (18)$$

So again it suffices to study the orientation of the MP problem. It is shown in figure 1. It is calculated at  $\varepsilon = 0.00005$  which is sufficiently small to guarantee that we are in the linear regime. The dominant feature is the linear behaviour in the bulk of the chain. Pulling a chain at the head will produce the largest orientations at the head, which gradually diminish towards the tail due to fluctuations. There exists a useful relation between the orientation of the end link and the drift velocity  $v$ , reading as [21]

$$\langle y_1 \rangle_{\text{EP}} = -\frac{2d\varepsilon}{2d+1} + v_{\text{EP}}, \quad v_{\text{MP}} = \frac{2dp_1}{2d+1}. \quad (19)$$

As we know the drift velocity, we can estimate the value  $p_1$  [9, 10]

$$p_1 \simeq \frac{1}{2dN^2}. \quad (20)$$

Formally one can extract the equation for the hopping tagged particle from the full master equation for  $P_j(\mathbf{x})$ . We define the hopping rates  $W_+(j)$  as

$$\begin{aligned} W_+(j)p(j) &= \sum_{\mathbf{x}} P_j(\mathbf{x})(1-x_{j+1}) \\ W_-(j)p(j) &= \sum_{\mathbf{x}} P_j(\mathbf{x})(1-x_{j-1}). \end{aligned} \quad (21)$$

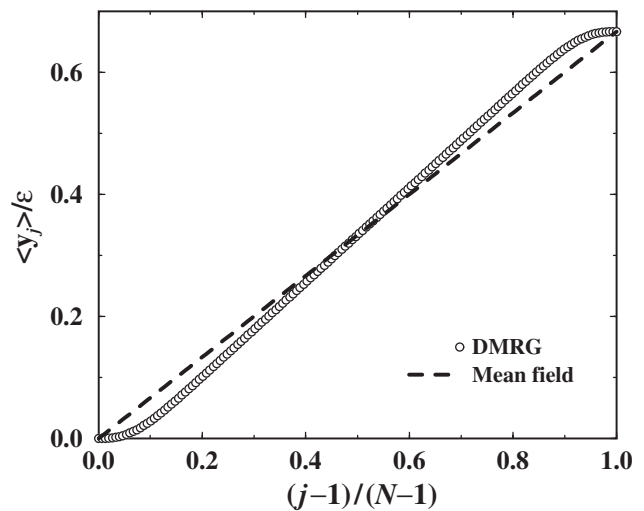


Figure 1. The MP orientation for  $N=150$  and  $d=1$ . The dashed line is the mean-field result (26).

Clearly  $W_+(j)$  is the conditional probability that the tag at  $j$  has a hole next to it at  $j+1$ . Thus it is the rate at which the tag hops from link  $j$  to link  $j+1$ . Similarly  $W_-(j)$  is the rate by which it jumps to  $j-1$ . This gives the general equation for  $p_j$

$$W_+(j-1)p_{j-1} + W_-(j+1)p_{j+1} = [W_+(j) + W_-(j)]p_j, \quad j \neq 1, N-1. \quad (22)$$

The difficulty is of course to find expressions for these hopping rates  $W_{\pm}(j)$ . The equations have a conserved current, which becomes clear by reorganizing them as

$$\left\{ \begin{array}{l} W_-(2)p_2 - W_+(1)p_1 = p_1, \\ W_-(3)p_3 - W_+(2)p_2 = W_-(2)p_2 - W_+(1)p_1, \\ \dots = \dots \\ W_-(N)p_N \\ -W_+(N-1)p_{N-1} = W_-(N-1)p_{N-1} \\ \quad - W_+(N-2)p_{N-2}, \\ p_1 = W_-(N)p_N - W_+(N-1)p_{N-1}. \end{array} \right. \quad (23)$$

Here we have included the special equations for the tail and head link. As the left-hand side of an equation appears as the right-hand side of the next equation, all the members of this set must be equal to  $p_1$ . Note that equations (23) are dependent (as can be seen by adding them all). Thus the set allows an arbitrary normalization which we take as

$$p_1 + p_N = 1. \quad (24)$$

It is consistent with the relation to the orientation (18).

In order to get a feel for this equation we make a mean-field assumption on the hopping rates  $W_{\pm}(j)$ . A particle can move to a neighbouring link when that is occupied by a vacancy. The uncorrelated probability on a vacancy is  $1/(2d+1)$ . Taking this as a measure for  $W_{\pm}(j)$  we arrive at the equations

$$p_{j+1} - p_j = (2d+1)p_1, \quad j \neq 1, N-1. \quad (25)$$

It is not difficult to solve the system (25), yielding the solution

$$p_j = \frac{(2d+1)j - 2d}{(2d+1)(N+1) - 4d}. \quad (26)$$

This approximation gives a straight increase from tail to head, which we have also drawn in figure 1. It gives

the illusion that the mean-field approximation does reasonably well in predicting the local orientation of the MP problem.

Formula (26), however misses the essence of the orientation of the EP problem. Translating (26) to the EP problem via

$$\langle y_j \rangle_{EP}/\epsilon = (N+1)\langle y_j \rangle_{MP}/\epsilon - \frac{2dj}{2d+1}, \quad (27)$$

gives the mean-field approximation for the EP chain

$$\langle y_j \rangle_{EP}/\epsilon = \frac{(2d)^2}{(2d+1)(2d+1)(N+1) - 4d} \cdot (2j - N - 1). \quad (28)$$

Note that the symmetry holds throughout the chain and not only for the end links, where it is enforced by (24). The plot for this orientation, as obtained from DMRG calculations, is quite different from the numerical data. Figure 2 shows a series of orientations for various lengths  $N$ . The dashed line gives the mean-field approximation. It shows the counter-intuitive feature that the longer the chain, the larger are the deviations from the mean-field approximation. The mean-field approximation fails in two respects: the slope is too small and independent of the length (when plotted as a function of  $j/N$ ), while the data give a slow increase with length. Also the initial and final value differ from the correct value in a way which is detrimental for the drift velocity. According to (26) we get  $p_1 \simeq 1/(2d+1)N$  while it should be an order of magnitude smaller in  $N$  in order to match the drift velocity given by (20).

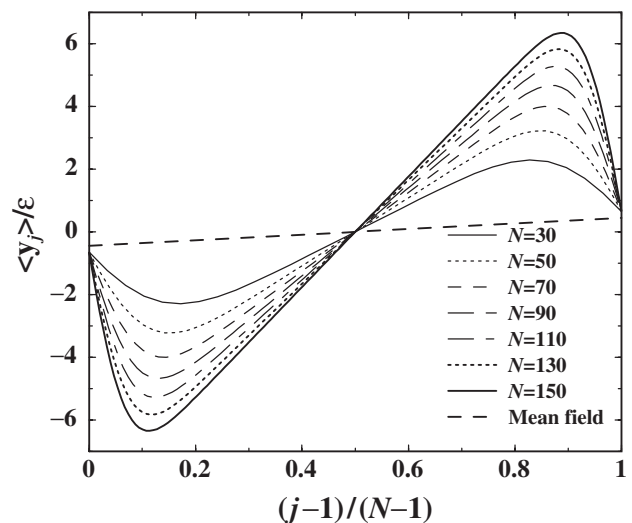


Figure 2. Profiles for a series of chains of length  $N=30$  to 150. The dashed line is the mean-field approximation (28).

#### 4. Scaling behaviour

The almost linear behaviour of  $p_j$  with  $j$  as shown in figure 1 is easily understood as a diffusion process of the tagged particle. When inserted at the head of the chain, it can do nothing else other than drift to the tail of the chain. The drift velocity equals  $p_1$  as this is the probability that the tag leaves the chain at the tail and is reinstalled at the head. For long chains we can turn the discrete equations (23) into a Fokker–Planck equation [22]

$$-\frac{d}{dj}[W_+(j) - W_-(j)]p_j + \frac{1}{2} \frac{d^2}{dj^2}[W_+(j) + W_-(j)]p_j = 0. \quad (29)$$

The sum  $W_+(j) + W_-(j)$  represents the diffusion coefficient and the difference  $[W_+(j) - W_-(j)]$  is the systematic force. The main error of the mean-field approximation of the previous section is that it ignores the systematic force. We can understand this force by viewing the random walk as a time-dependent process. Then the probability  $p_j$  can be interpreted as the residual time of the tag at link  $j$ . Thus the tag spends most of its time at the head and dramatically less (2 orders of magnitude in  $N$ ) at the tail of the chain. Since the current is a constant along the chain, the tag proceeds (on the average) slowly at the head and fast at the tail. This explains why the surrounding around the tag is in equilibrium near the head, with almost equal probabilities to move to right or left. But near the tail the tag moves fast and creates a surplus of particles at its tail side and a depletion of particles (or an accumulation of holes) at its head side. This causes the imbalance in the jump rates near the tail. The lack of holes at the tail side makes  $W_-(j)$  smaller than average and the surplus of holes at the head side increases the value of  $W_+(j)$ .

We can make this qualitative argument more quantitatively in the bulk of the chain. If we move with the average position of the tag in a run from head to tail, we encounter a steady increase of  $W_+(j)$  ahead of the tag and a decrease of  $W_-(j)$  behind the tag. The effect will be proportional with the velocity of the tag and therefore inversely proportional with  $p_j$ , which roughly grows with the position  $j$ . So we have to leading order

$$W_+(j) - \frac{1}{2d+1} \simeq \frac{g^+}{j}, \quad \frac{1}{2d+1} - W_-(j) \simeq \frac{g^-}{j}. \quad (30)$$

This simple observation already implies an important result: correlations as incorporated in the deviation of the  $W_{\pm}(j)$  from random, decay algebraically as a function of the position.

Relation (30) can be articulated further by using the symmetries, as following from (13) and (15)

$$p_j + p_{N+1-j} = 1, \quad W_+(j)p_j + W_{N+1-j}p_{N+1-j} = \frac{1}{2d+1}. \quad (31)$$

So in the middle of the chain  $p = 1/2$  and the sum  $W_+ + W_- = 2/(2d+1)$ . Combining this with the Fokker–Planck equation (29) and the requirement of linearity of  $p_j$  (which is the input of (30)) gives for the bulk values  $g^{\pm}$

$$g^{\pm} = \frac{1}{2(2d+1)}. \quad (32)$$

The DMRG calculations provide us directly with the functions  $W_{\pm}(j)$ . DMRG gives, apart from the orientation, also the joint probabilities for 2 consecutive links. Now the combination  $W_-(j)p(j)$  is the joint probability to find the tag on link  $j$  and a hole on link  $j-1$ , as can be seen from its definition (21). Therefore we have this combination as a correlation function in the DMRG calculation of the MP model. The most accurate measurement, at the moment, is the EP model at very small  $\varepsilon$ . But these values can be translated with the general relation (6) between models.

In figure 3 we show the rates  $W_{\pm}(j)$  for  $N=150$  (and  $d=1$ ). Clearly the deviations from  $1/(2d+1)$  are the largest at the tail of the chain. These deviations stay when the chain gets longer, just as (30) predicts. However the numerical values are not correct, which is not surprising since (30) refers to the bulk. The increase

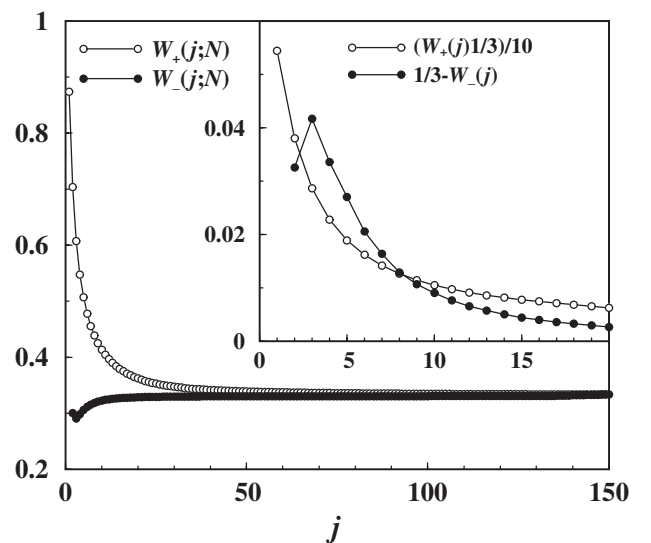


Figure 3. Transition rates  $W_{\pm}(j)$  for  $N=150$  and  $d=1$ . The inset shows the values near the tail, extrapolated to  $N = \infty$ .

of  $W_+(j)$  is larger and the decrease of  $W_-(j)$  is smaller than expression (30).

The size of the region where deviations of (30) become important can be estimated as follows. Assume that it is a region of order  $N^\alpha$ . Then we expect a correction to (30) of the type

$$g(x) = g^+(x) + g^-(x) = \frac{1}{2d+1} + g_{-1} \frac{1}{x} + \dots, \quad x = \frac{j}{N^\alpha}. \tag{33}$$

Inserting this into the Fokker–Planck equation (30) we get a refinement of the linear behaviour of  $p_j$  in the middle of the chain

$$p_j = \left(1 + \frac{(2d+1)g_{-1}}{N^\alpha}\right) \frac{j}{N} - \frac{(2d+1)g_{-1}}{2N^\alpha}. \tag{34}$$

The slope is increased by a small amount, which induces an offset by the same amount, in order to preserve the value  $p = 1/2$  in the middle. Then extrapolating (34) backwards to the point where  $p_j$  gets vanishingly small, we find a value

$$j \sim (2d+1)g_{-1}N^{1-\alpha}/2. \tag{35}$$

This must be of the same order as the assumed range  $N^\alpha$ , implying that  $\alpha = 1/2$ . Thus the scale of the tail region is of the order  $N^{1/2}$ .

This is confirmed in figure 4, where we plot the systematic force multiplied by  $j$ . We observe that the scaling form

$$[W_+(j) - W_-(j)] \simeq \frac{g(x)}{j}, \quad x = \frac{j}{N^{1/2}}, \tag{36}$$

holds over practically the whole range of the chain, with the exception of the regions close to head and tail. In the subsequent figure 5 and 6, where we plot the same scaling function for the embedding dimensions  $d=2$  and  $d=3$ , we see that the asymptotic behaviour as predicted by (30) is well obeyed. That the curves start to fan out at the head is simply the effect of the finiteness of the chains. For longer and longer chains, scaling would extend over a longer and longer range.

More delicate is the scaling behaviour for small argument. In [18] we concluded to the value  $g(0) = 3/(2d+1)$ , on the basis of an integration of the Fokker–Planck equation from a point  $x_0$ , where the scaling starts to hold, up to the middle of the chain. Scaling cannot hold all the way down to the tail, as it predicts a variation of  $g$  on the scale of  $N^{1/2}$  while the  $W_\pm(j)$  vary from link to link, as the inset of figure 1 shows. For  $N \rightarrow \infty$  a link  $j_0$

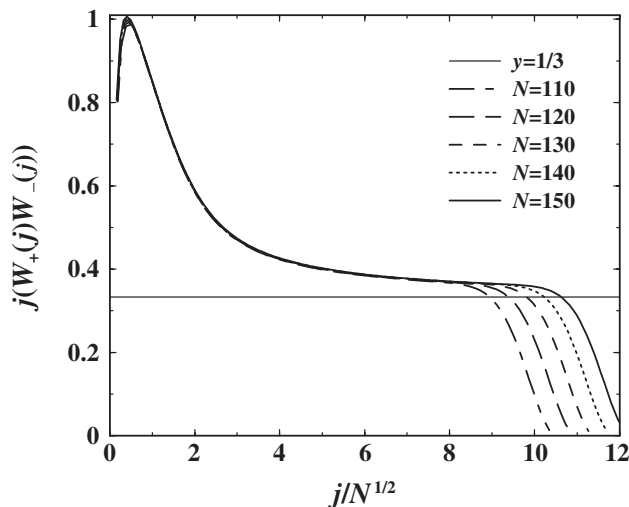


Figure 4. The scaling form for the systematic force,  $d=1$ . The horizontal line gives the asymptote  $1/(2d+1)$ .

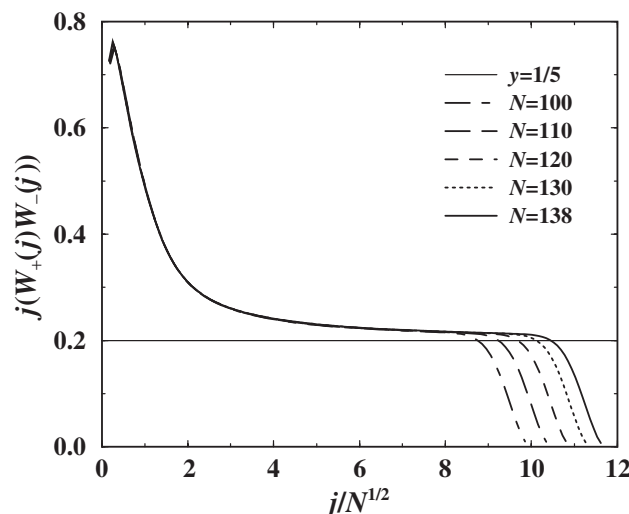


Figure 5. The scaling form for the systematic force,  $d=2$ . The horizontal line gives the asymptote  $1/(2d+1)$ .

can be found with  $j_0 \gg 1$  and  $j_0 \ll N^{1/2}$  such that  $x_0 = j_0/N^{1/2} \rightarrow 0$ . The chains for which we could perform the DMRG calculations are not sufficiently long to demonstrate this limit, as the figures show.

The values of  $W_\pm(j)$  near the tail cannot be obtained from a continuum approach such as the Fokker–Planck equation (30). A ‘microscopic’ calculation can be made considering the complex of a tag and an adjacent hole as a new random walker. To illustrate the principle, consider  $W_+(1)$ , referring to the situation where the tag sits at link 1 and a hole at the adjacent link 2. We now take also the hole as marked and speak about it as a vacancy. The background for the tag and vacancy

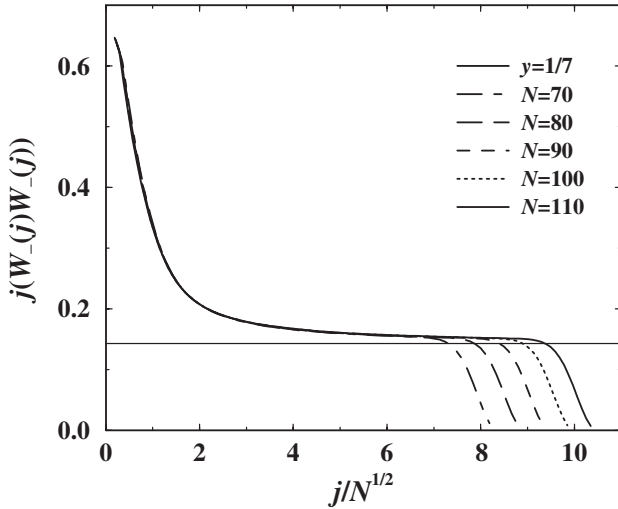


Figure 6. The scaling form for the systematic force,  $d=3$ . The horizontal line gives the asymptote  $1/(2d+1)$ .

are formed by particles and holes. We study the combined drift of tag and vacancy. With the tag at link 1, it has the option to jump to the head of the chain or to exchange with the vacancy. Both processes have a transition rate 1. The vacancy can hop into the chain by exchange with particles. This creates a series of states

$$t_0 = (tv\dots), \quad t_1 = (t1v\dots), \quad t_2 = (t11v\dots), \dots, \quad (37)$$

where the dots  $\dots$  inside the brackets stand for an arbitrary further occupation. We name these objects ‘states’ because they consist of many configurations. The links between the tag and the vacancy we call the inside region; the  $\dots$  refer to the outside region. All the states prevent the tag from moving into the chain, except  $t_0$ . The transition rates to lower values of  $n$  are all 1, but we do not know the transition rates upstream. In the spirit of (26) we assume them to be  $q \simeq 2d/(2d+1)$ , being the ‘equilibrium’ density of particles in the outside region. So the general equation reads

$$(1+1+q)t_n = t_{n+1} + qt_{n-1}, \quad n > 0. \quad (38)$$

It has the solution

$$t_n = t_0 x^n, \quad x = 1 + q/2 - (1 + (q/2)^2)^{1/2}. \quad (39)$$

We have to take the negative root of the quadratic equation since it is smaller than 1 and the other is larger than 1. For  $q = 2/3$  the value of  $x$  is slightly smaller

Table 1. Approximate and exact transition rates  $W_{\pm}$  for  $N = 10$ .

$j$	$W'_+(j)$	$W'_-(j)$	$W_+(j)$	$W_-(j)$
1	0.7208	–	0.8374	–
2	0.5365	0.2952	0.6180	0.2993
3	0.4694	0.2718	0.4953	0.2832
4	0.4346	0.2749	0.4260	0.2862
5	0.4139	0.2801	0.3870	0.2904
6	0.3982	0.2841	0.3644	0.2944
7	0.3824	0.2882	0.3505	0.2995
8	0.3636	0.2949	0.3413	0.3074
9	0.3408	0.3054	0.3351	0.3183
10	–	0.3221	–	0.2392

than  $1/3$ . The smaller  $q$ , the smaller  $x$ . For the rate  $W_+(1)$  we thus find

$$W_+(1) = t_0 / \sum_{n=0}^{\infty} t_n = 1 - x. \quad (40)$$

For  $q = 2/3$  transition rate  $W_+(1)$  equals 0.72. This is significantly higher than the uncorrelated value  $1/3$ .  $q$  is the probability to find a particle next to the vacancy, while  $x$  is, according to (40), the probability to find a particle next to the tag. The only approximation made in deriving (40) is the assumption of a constant rate  $q$  for the exchange of the vacancy with particles on the head side of the vacancy. Interpreting  $x$  as the particle density left of the tag, one would take for  $q$  a value somewhere in between the value  $x$ , which is significant near the tag, and  $2d/(2d+1)$ , which holds far away from the tag. This would enforce the effect by lowering  $x$  further.

One can extend the scheme to the other values of  $W_{\pm}(j)$ . We outline this in the appendices. In table 1 we show the results for a chain with  $N=10$ . The table shows that the trends are correct. In fact extending the calculation for long chains one finds a behaviour similar to (36), i.e. algebraic decay and scaling. Again the mean-field hopping rates, assumed for the hops of the tag and the vacancy extending their distance, does not produce scaling functions with the proper limits.

## 5. Conclusion

We have used the magnetophoresis model as the central ingredient in understanding the reptation profiles of the Rubinstein–Duke model with arbitrarily charged reptons. In the weak field limit the probability distribution of the general case can be rigorously expressed

in terms of  $P_j(\mathbf{x})$  (of the MP model) by relation (6).  $P_j(\mathbf{x})$  is interpreted as the probability of finding a marked link  $j$  (a tag) in a configuration  $\mathbf{x}$ . The orientation of the MP model is given by the probability of finding the tag, which runs from head to tail and then jumps back to the head. Hopping rates for the tag follow from the contracted master equation for the tag. These transition rates  $W_{\pm}(j)$  are determined with the DMRG method, which we have used to solve the master equation. Near the tail, the transition rate  $W_{+}(j)$ , for a jump away from the tail, is considerably larger than the random value  $1/(2d+1)$ , which nearly holds in the bulk of the system. Similarly the rate  $W_{-}(j)$ , for a jump to the head side, is below the random value, close to the tail. Asymptotically the rates decay algebraically towards the bulk values beyond a tail regime of size  $N^{1/2}$ . These basic properties, algebraic decay and scaling, are derived from a general physical picture. Detailed calculation for the rates  $W_{\pm}(j)$  are performed by viewing the tag–vacancy combination as a new random walker. Whereas the tag hops along a linear domain, the tag–vacancy complex hops in a two-dimensional space. Taking the transition rates for these complex random walkers as random, leads to values which qualitatively agree with the measured values for the  $W_{\pm}(j)$  (see table 1). They demonstrate for long chains the scaling behaviour given in (36) but the scaling functions are rather different. It means that scaling and algebraic decay are robust features, but the form of the scaling function is sensitive to the hopping rates for the tag–vacancy complex.

One could proceed by considering higher complexes, to improve the rates for the tag–vacancy walker, but this becomes rapidly unwieldy. More promising is to make the rates self-consistent with the results of the calculation. Indeed preliminary calculations give an improvement, but the calculation of this self-consistent value for long chains becomes lengthy. Moreover a scaling function only yields a quantitatively correct orientation if the asymptotic limits as given by (30) are reproduced and one cannot expect to get these values correct by making approximations with a mean-field flavour.

The fact that the chain has at its ends domains of the size  $N^{1/2}$  is a general manifestation of the large influence of finite size corrections and that global properties have to be analysed as a function of  $1/N^{1/2}$ . This is confirmed by the finite-size analysis of the renewal time and diffusion coefficient [16]. The algebraic decay towards bulk behaviour shows that the stationary state of a drifting long polymer is ‘critical’, with algebraic rather than exponential decay–correlations, rendering mean-field approximations

useless. This contrasts with the static properties, for which the length on the polymer tends to justify a mean-field approximation.

### Acknowledgements

This work has been supported by the Polish Science Committee (KBN) through Grant No. 2 P03B 125 24. AD wants to thank CELTAM (Center for Low Temperature Studies of Promising Materials for Applications) in Poland for financing his research visit at Leiden.

### Appendix A: Calculation of $W_{+}(j)$

Before we extend the calculations of the  $W_{\pm}(j)$  other  $W_{+}(1)$ , we want to point out that we have not used the equation for the value of  $t_0$ . For this equation we have to know the exchange with the configuration  $(vt\dots)$ . There is a flow from  $(vt\dots)$  to  $(tv\dots)$  which is known from global considerations. The strength of this flow determines the magnitude of the series  $t_n$ . We could calculate the ratio  $W_{+}(1)$  without using the flow. It is also important that the jump of the tag from link 1 to  $N$  has no inverse process, as we will see in the discussion of the  $W_{-}(j)$ .

The next quantity to consider is  $W_{+}(2)$  from which the general pattern will become clear. In analogy with (37) we consider the series

$$\begin{aligned} (\cdot t)_0 &= (\cdot tv\dots), & (\cdot t)_1 &= (\cdot t1v\dots), \\ (\cdot t)_2 &= (\cdot t11v\dots), \dots \end{aligned} \quad (\text{A1})$$

Now, not only the vacancy can drift away from the tag, but the tag can also drift away from the vacancy, albeit only over one step. Thus we include the series

$$\begin{aligned} (t0)_0 &= (t0v\dots), & (t0)_1 &= (t01v\dots), \\ (t0)_2 &= (t011v\dots), \dots \end{aligned} \quad (\text{A2})$$

The characteristic of the configuration  $(t0)_n$  is that there are  $n$  particles and one hole in the inside region. This hole may move around in the inside region, without changing the position of tag and vacancy. It seems therefore reasonable to change the definition (A2) to

$$\begin{aligned} (t0)_n &= (\overline{t0\dots}) = (t01\dots v) + (t10\dots v) \\ &\quad + \dots + (t1\dots 0v), \end{aligned} \quad (\text{A3})$$

where the overline indicates that all the distributions of particles and holes have to be taken and where the  $\dots$  stand for particles. It means that we take the inside region to be in equilibrium for given positions of the tag and the vacancy.

Next we have to settle the transition rates between these states. As before we assume that the exchange of the vacancy against a particle on the outside goes with the rate  $2d/(2d+1)$ . Similarly we take for the exchange rate of the tag with a hole outside the value  $1/(2d+1)$ . For the hopping rates shrinking the inside region we take the equilibrium values. Thus we assume  $n/(n+1)$  for the vacancy and  $1/(n+1)$  for the tag. The rates are simply the densities of the particles, namely, holes in the states participating in the transition. This settles the flow pattern. We have the global flow from configuration  $(\cdot vt \dots)$  to the configuration  $(\cdot t)_0$ , which sets the magnitude of the probabilities. The configurations of the series (A2) all have an outflow rate of 1 and no corresponding inflow. The rate  $W_+(2)$  is then given as

$$W_+(2) = \frac{(\cdot t)_0}{\sum_n (\cdot t)_n}. \quad (\text{A4})$$

The general case  $W_+(j)$  follows from letting the tag move to the tail with rate  $1/(2d+1)$  and the vacancy with rate  $2d/(2d+1)$  each to its end of the chain. In the opposite direction we take the rates for shrinking the inside region as the density of holes for the tag and that of the particles for the vacancy. The densities are determined as the fraction of the number of participating states that qualify. There is one new element in the game that becomes more important when  $j$  grows. In general the vacancy drifts with  $2d$  times the speed of the tag to its end of the chain, in this case the head. So for  $j$  beyond the fraction  $1/(2d+1)$  of the chain, the vacancy has reached the head and disappears from the chain, before the tag reaches the tail. If we were to stop the inclusion of states at that point, the tag would still grow more holes in the inside region and we would miss the important configurations having a ratio 1 to  $2d$  of holes to particles. So we must allow particles to come in from the head side to obtain the right mix of holes and particles for the states where the tag is close to the tail. This effect becomes dramatic for values of  $j$  near the head. Take the extreme case  $W_+(N-1)$ . The vacancy sits at the head link and has as its only option to disappear, while the tag may run over  $N-2$  links before the tail is reached. The final states then would have  $N-2$  holes versus at best one particle. These states are totally irrelevant for the process. So we have to include configurations with

more particles, by growing them from the head side. For the configurations where the tag is located at link  $k$  we include all states with no vacancy and number of particles up to  $N-k$  (which is also an unrealistic overkill). Tableau (B7) elucidates this point.

## Appendix B: Calculation of the $W_-(j)$

The calculation of the rates  $W_-(j)$  is more difficult because we have to determine the inflow at the head side, which is less clear than the outflow at the tail side. Let us again start the discussion with the simplest case  $W_-(N)$ , which refers to the tag at link  $N$  and the vacancy next to it at link  $N-1$ . The tag cannot leave at the head side; it can only exchange position with the vacancy. The vacancy may drift to the tail at a rate  $q = 2d/(2d+1)$ . So we get the sequence of states

$$s_0 = (\dots vt), \quad s_1 = (\dots v1t), \quad s_2 = (\dots v11t), \dots \quad (\text{B1})$$

Note that these states are the transposition of the states  $t_n$  of (37). All the states  $s_i$  receive an influx of the corresponding transposed state  $t_n$  with rate 1. In addition the state  $s_0$  may change into  $(\dots tv)$  to which we give a weight  $z$ . So we obtain the general equations

$$(1+q)s_n = s_{n+1} + qs_{n-1} + t_n, \quad i > 0. \quad (\text{B2})$$

The case  $n=0$  is special with  $qs_{n-1}$  replaced by  $z$ . The set of equations is satisfied by the ansatz

$$s_n = Ax^n + Bq^n, \quad (\text{B3})$$

where  $x$ , given by (39), is the power by which the  $t_n$  decay. The value of  $A$  follows by matching the terms with the same power of  $x$  and leads to  $A = x - 1$ . The value of  $B$  follows from the special equation  $n=0$ . The algebra gives the expression for  $W_-(N)$

$$W_-(N) = \frac{(q-x)(1-x) + z + t_0}{(q-x)(2-x) + z + t_0} (1-q). \quad (\text{B4})$$

The value of  $z$  entering in the expression has to be obtained from the calculation of  $W_+(N-1)$ , outlined in the previous section. Also we used the solution of the problem of  $W_+(1)$ . The value of  $z$  tends towards large values in our normalization for large  $N$ . This explains why  $W_-(N)$  tends (from below) to the random value  $1-q = 1/(2d+1)$  for long chains.

For the general case let us start at the state where the tag is at position  $j+1$  and the vacancy at  $j$ , which is the starting state for the problem  $W_-(j+1)$ . One option

for this state is that the tag moves upstream towards the head and the vacancy downstream to the tail. These are fluctuations against the mainstream. The other option is that the state interchanges tag and vacancy, which is the initial situation for the problem to calculate  $W_+(j)$ . Following the diffusion of the tag and the counterflow of the vacancy in this sector, we end up with states where the tag is at the tail. These states jump to the transposed configurations with the tag at the head and the vacancy (if present) at the tail side. To be precise: these are the states belonging to the problem  $W_-(N-j)$ . Thus in this sector the tag trickles down to the position  $N-j$ . At this point it may meet the vacancy of the sector and exchange with it, assuming the position  $N-j-1$ . Clearly we then have moved to the sector of  $W_+(N-j-1)$ . Then again the tag starts to flow down to the tail and flips to the head. It enters the sector of the  $W_-(j+1)$  states and we are back to the original problem. Ergo 4 sectors are involved in the sequence

$$\begin{aligned} W_-(j+1) &\Rightarrow W_+(j) \Rightarrow W_-(N+1-j) \Rightarrow W_+(N-j) \\ &\Rightarrow W_-(j+1). \end{aligned} \quad (\text{B5})$$

As an illustration of the flow pattern we give in tableau (B7) the explicit example of  $N=5$  where we start at sector  $W_+(2)$ .

The flow between every two consecutive sectors is equal to the total flow  $J$ , which we have put equal to 1 in the calculation of the states in the  $W_+$  problems. For a  $W_-$  to a  $W_+$ , the flow is by interchange of tag and vacancy. For the jump from a  $W_+$  to a  $W_-$  the flow is a flip from tail to head. By setting  $J=1$ , we have made a normalization such that the total probability of the tag being at the tail is set to 1 (whereas it should be the much smaller  $p(1)$ ). As we focus on rates, which are ratios, we do not care about normalization. The values of the  $W_+$  problem serve as input for the  $W_-$  problem in two ways:

- the  $W_-(j)$  problem gets the influx of the  $W_+(N+1-j)$  states with the tag at the tail, to the  $W_-(j)$  states with the tag at the head;
- the state  $(\dots vt \dots)$  of  $W_-(j)$  is connected to the state  $(\dots tv \dots)$  of  $W_+(j-1)$  by the relation ( $J=1$ )

$$(\dots vt \dots) = (\dots tv \dots) + 1. \quad (\text{B6})$$

The moral of the story is that we must first calculate 2 problems  $W_+(N-j)$  and  $W_+(j-1)$  in order to determine the input for the problems  $W_-(N-j+1)$  and  $W_-(j)$ . In order to illustrate the flow pattern we give the explicit example of  $N=5$  where we start at the sector of  $W_+(2)$ . The double updownarrows stand for the flow  $J$ . We have made this arrow doubly pointed

to indicate that the flow is the result of back and forth processes. The single downarrows in a row also carry together the current  $J$ . They are singly pointed as the flow is only in one direction. In fact the total flow from one row to the next equals  $J$  for all the rows in the scheme. The bottom updownarrow flows again to the first state of the top row.

$$\begin{array}{cccccc} W_+(2): & (\cdot tv \cdot \cdot) & (\cdot t1v \cdot) & (\cdot t11v) & (\cdot t111) & \\ & (t0v \cdot \cdot) & (t\overline{0}1v \cdot) & (t\overline{0}11v) & (t\overline{0}111) & (t1111) \\ & \downarrow & \downarrow & \downarrow & \downarrow & \downarrow \\ & (\cdot \cdot v0t) & (\cdot \cdot v\overline{0}t) & (v\overline{1}10t) & (\overline{1}110t) & (1111t) \\ W_-(4): & (\cdot \cdot vt \cdot) & (\cdot v1t \cdot) & (v11t \cdot) & (111t \cdot) & \\ & \Downarrow & & & & \\ W_+(3): & (\cdot \cdot tv \cdot) & (\cdot \cdot t1v) & (\cdot \cdot t11) & & \\ & (\cdot t0v \cdot) & (\cdot t\overline{0}1v) & (\cdot t\overline{0}11) & (\cdot t111) & \\ & (t00v \cdot) & (t\overline{0}01v) & (t\overline{0}011) & (t\overline{0}111) & (t1111) \\ & \downarrow & \downarrow & \downarrow & \downarrow & \downarrow \\ & (\cdot v00t) & (v\overline{1}00t) & (\overline{1}100t) & (\overline{1}110t) & (1111t) \\ & (\cdot v0t \cdot) & (v\overline{1}0t \cdot) & (\overline{1}10t \cdot) & (111t \cdot) & \\ W_-(3): & (\cdot vt \cdot \cdot) & (v1t \cdot \cdot) & (11t \cdot \cdot) & & \\ & \Downarrow & & & & \end{array} \quad (\text{B7})$$

To calculate the elements of this scheme we first determine the sectors  $W_+(2)$  and  $W_+(3)$ , using an inflow at the top left corner  $J=1$ . This automatically normalizes the last row of the sectors. Then for the sector  $W_-(4)$  we have a known input (right hand side) at the top from the solution of sector  $W_+(2)$ .

## References

- [1] B. Widom, J.-L. Viovy, A.D. Defontaines. *J. phys. I*, **1**, 1759 (1991).
- [2] P.G. de Gennes. *Scaling Concepts in Polymer Physics*, Cornell University Press, Ithaca (1971).
- [3] M. Doi, S.F. Edwards. *The Theory of Polymer Dynamics*, Oxford University, New York (1989).
- [4] M. Rubinstein. *Phys. Rev. Lett.*, **59**, 1946 (1987).
- [5] T.A.J. Duke. *Phys. Rev. Lett.*, **62**, 2877 (1989); *J. chem. Phys.*, **93**, 9049 (1990); *J. chem. Phys.*, **93**, 9055 (1990).
- [6] G.T. Barkema, J.F. Marko, B. Widom. *Phys. Rev. E*, **49**, 5303 (1994).
- [7] G.T. Barkema, M.E.J. Newman. *Physica A*, **244**, 25 (1997); M.E.J. Newman, G.T. Barkema. *Phys. Rev. E*, **56**, 3468 (1997).
- [8] J.M.J. van Leeuwen, A. Kooiman. *Physica A*, **184**, 79 (1992).
- [9] A. Kooiman, J.M.J. van Leeuwen. *Physica A*, **194**, 163 (1993).
- [10] M. Prähofer, H. Spohn. *Physica A*, **233**, 191 (1996); M. Widom, I. Al-Lehyani. *Physica A*, **244**, 510 (1997).
- [11] B. Derrida, M. Evans, V. Hakim, V. Paquier. *J. phys. A*, **26**, 1493 (1993).

- [12] G.M. Schütz. In *Phase Transitions and Critical Phenomena*, C. Domb, J. Lebowitz (Eds), Vol. 19, Academic, London (2000).
- [13] S.R. White. *Phys. Rev. Lett.*, **69**, 2863 (1992); *Phys. Rev. B*, **48**, 10345 (1993).
- [14] I. Peschel, X. Wang, M. Kaulke, K. Hallberg (Eds). *Lectures Notes in Physics*, Vol. 528, Springer, Berlin (1999).
- [15] E. Carlon, A. Drzewiński, J.M.J. van Leeuwen. *Phys. Rev. E*, **64**, 010801(R) (2001).
- [16] E. Carlon, A. Drzewiński, J.M.J. van Leeuwen. *J. chem. Phys.*, **117**, 2435 (2002).
- [17] A. Drzewiński, E. Carlon, J.M.J. van Leeuwen. *Phys. Rev. E*, **68**, 061801 (2003).
- [18] A. Drzewiński, J.M.J. van Leeuwen. *J. stat. Mech.*, P02004 (2005).
- [19] G.T. Barkema, G.M. Schütz. *Europhys. Lett.*, **35**, 139 (1996).
- [20] M. Peassens. *J. chem. Phys.*, **118**, 10287 (2003).
- [21] A. Kooiman. On the Interface between two Coexisting Phases and Reptation Models for Electrophoresis. PhD Thesis, University of Leiden (1992).
- [22] N.G. van Kampen. *Stochastic Processes in Physics and Chemistry*, North Holland Publishing Company, Amsterdam (1981).